High-Resolution Neural Temperature Sensor Using Fiber Bragg Gratings

Shyh-Lin Tsao, *Member, IEEE,* Jingshown Wu, *Member, IEEE,* and Bih-Chyun Yeh

***Abstract*—We demonstrate a novel high-resolution neural temperature sensor using two fiber Bragg gratings (FBG's) and a modular artificial neural network which is used to learn the mapping relation among frequency, temperature, and the normalized transmission power spectrum. Because of the fast computational ability of the modular artificial neural network and the sensitivity of FBG's, the sensor can make high-resolution temperature and frequency measurements in real time. The experimental results show that the temperature resolution of this sensor can reach 0.005 °C.**

***Index Terms*—Feedforward neural networks, fiber Bragg gratings, fuzzy neural networks, temperature sensor.**

I. Introduction

Over the past ten years, most of the reported fiber Bragg grating (FBG) sensors used the phenomenon of power spectrum drifting with temperature to detect temperature variations [1], [2]. The dependence between the temperature and the Bragg wavelength caused by thermal expansion of the fiber and change of the refractive index in the core can be theoretically predicted and experimentally verified. Based on the amount of wavelength shift, the magnitude of the temperature variation can be deduced. Therefore, measurement of the wavelength shift is a key issue for in-fiber Bragg-grating sensors. Several sensing schemes, such as the edge filter, tunable filter, and interferometric scanning method, have been proposed to measure the degree of wavelength shift of an FBG [3]–[8]. Some experiments using CCD spectrometers have also been reported in the literature with promising results. A CCD line array with a holographic grating can be fixed in a mechanical breadboard [9], [10]. However, these schemes utilize either the entire power spectrum of the FBG or phase detection to identify the degree of wavelength shift. There are three general requirements for a useful sensor: 1) good resolution with enough measurement range; 2) cost effectiveness; and 3) compatibility with multiplexing. According to these requirements, we must design a fiber sensor with the benefits of artificial neural networks.

In many practical cases, the amount of raw data is huge and, most of the time, is difficult to interpret. Artificial neural networks (ANN's), which have self-learning ability and are trainable to interpret raw data, are good information processing tools. In recent years, some ANN's have been applied to sensing systems [11]–[15]. ANN's are used to learn the functional mapping relationship from the raw data to the physical quantities. Based on the characteristics of ANN's, they can be classified as supervised methods (classification [13] or regression [11], [14]) and unsupervised methods [15]. These neural processing type sensors, based on the general ability of the trained ANN's, can achieve high resolution and accuracy. Sensors with ANN's can be implemented directly by using parallel computation chips to process distributed signals in real time.

In this paper, we propose a novel neural FBG temperature sensor, which combines the features the good sensitivity of FBG sensors and real neural processing. This sensor improves the sensing speed and accuracy, reduces cost, and eliminates the process of scanning over the entire power spectrum of the FBG. In the future, fiber optics and small-size neural networks will potentially make the integration of sensing, training, and processing functions in one compact smart apparatus feasible. The remainder of this paper is organized as follows. In Section II, the modular ANN used to learn the many-to-one mapping relationship is described. The sensing principle and procedures are discussed in Section III. The experimental setup and the results, which demonstrate that resolution as high as 0.005 °C can be achieved, are both presented in Section IV. Finally, the conclusions are given in Section V.

II. Modular Artificial Neural Network

In this paper, we use a modular artificial neural network which combines a multi-layer perceptron (MLP), ANN's [16], and a fuzzy network [17], [18] to learn a two-input-to-one-output mapping as

$$RT = S(M_1, M_2) \tag{1}$$

where RT is the detected response of the sensors, (M_1, M_2) are the physical quantities to be measured in the environment, and $S(\cdot)$ represents the mapping function of the sensor from (M_1, M_2) to RT. The MLP ANN is a powerful tool for information processing, but the weights of the MLP ANN cannot be determined easily. However, the fuzzy network has the capability of managing the parameters of a physical system. The parameters of the fuzzy network can be initialized by using *a priori* knowledge to shorten the training process. Therefore, we combine the MLP ANN's and the fuzzy network

Manuscript received September 18, 1998; revised May 25, 1999, and July 28, 1999. This work was supported in part by the National Science Council under Contract NSC 87-2215-E-155-003 and Contract NSC 87-2732-E-002-001.

S.-L. Tsao is with the Department of Electrical Engineering, Yuan Ze University, Chung-Li, Taiwan 320, R.O.C.

J. Wu and B.-C. Yeh are with the Department of Electrical Engineering, National Taiwan University, Taipei, Taiwan 10617, R.O.C.

Publisher Item Identifier S 0018-9197(99)06779-2.

0018–9197/99$10.00 © 1999 IEEE

Authorized licensed use limited to: National Taiwan University. Downloaded on January 23, 2009 at 00:46 from IEEE Xplore. Restrictions apply.

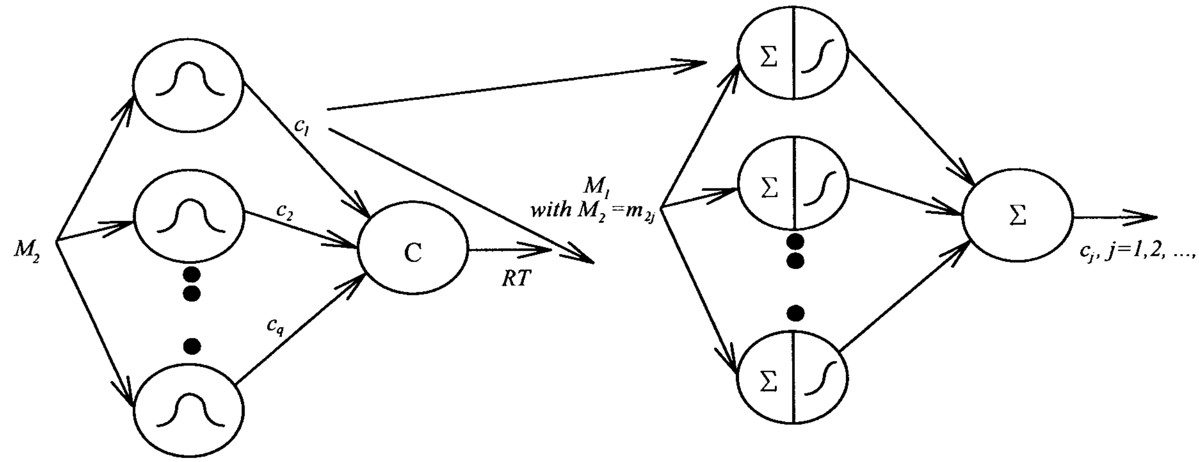

Fig. 1. The signal flow chart of the modular ANN.

as a modular ANN to learn the nonlinear mapping functions. This modular ANN is a network containing localized computation nodes in which each module is an independent system interacting with other modules to perform a more complex function.

The architecture of the modular ANN is illustrated in Fig. 1. The fuzzy network as depicted by the left side of Fig. 1 can be trained to learn the mapping relationship from M_2 to RT as follows:

$$RT = \frac{\sum_{j=1}^{q} c_j^* \mu_{m_{2j}}(M_2)}{\sum_{j=1}^{q} \mu_{m_{2j}}(M_2)} \tag{2}$$

and

$$\mu_{m_{2j}}(M_2) = \exp\left[-\left(\frac{M_2 - m_{2j}}{\sigma_j}\right)^2\right] \tag{3}$$

where RT is the output of the modular ANN, $\mu_{m_{2j}}(\cdot)$ is the jth membership function of the linguistic descriptions of the input variable M_2, c_j is the output of the jth MLP ANN, and m_{2j} and σ_j, with $j = 1, 2, \cdots, q$, are the adjustable parameters of the fuzzy network.

The MLP ANN is trained to learn the mapping relationship from M_1 with $M_2 = m_{2j}$ to c_j, as shown by the right side of Fig. 1. The symbol Σ represents an adaptive linear combiner (ALC), which simply performs a weighted sum of the input with a bias term as in the following expression:

$$y = \sum_{i=1}^{P} x_i w_i + w_o = \boldsymbol{X^T W} + w_o \tag{4}$$

where y is the output of the ALC, $\boldsymbol{X}$ is an input vector of the ALC, $\boldsymbol{W}$ is a weighting vector of the ALC, and w_0 is the bias term. The symbol $\int$ in Fig. 1 represents an activation transfer function, which calculates the output of the node with the weighted input signal (the output of the ALC). We use the hyperbolic tangent function $\tanh(\cdot)$ as the activation transformation. Therefore, we can train each submodel in the modular ANN separated by the back-propagation algorithm [19]. Each M_1 with $M_2 = m_{2j}$ maps to the submodel of c_j and then M_2 maps to the submodel of RT.

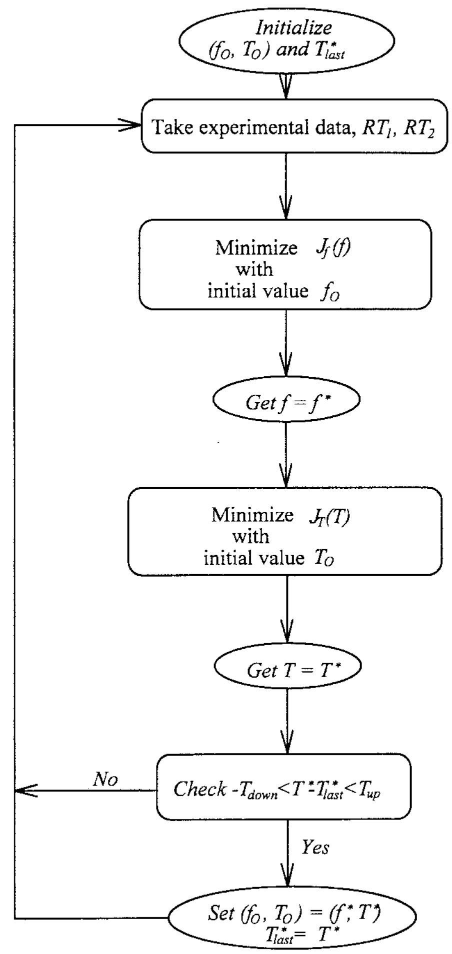

Fig. 2. The sensing procedure.

For simplicity, we denote each submodel by the same functional form as

$$y = fneu(x, \boldsymbol{W}) \tag{5}$$

where y is the output of a submodel, x is the input of the submodel, and $\boldsymbol{W}$ is a vector representing the adjustable

Authorized licensed use limited to: National Taiwan University. Downloaded on January 23, 2009 at 00:46 from IEEE Xplore. Restrictions apply.

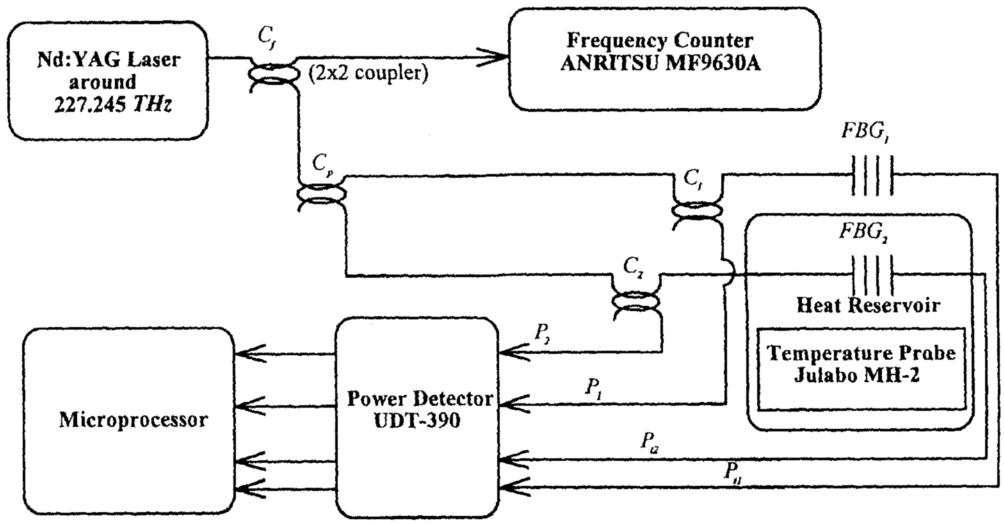

Fig. 3. The experimental setup.

weights of the submodel. Then, for a given training set, $(x_i, y_i), i = 1, 2, \cdots, N$, we define the sum square error function as

$$E(\boldsymbol{W}) = \frac{1}{2} \sum_{i=1}^{N} (y_i = fneu(x_i, \boldsymbol{W}))^2. \tag{6}$$

Based on the back-propagation algorithm, the weight vector $\boldsymbol{W}_{k+1}$ can be adjusted as

$$\boldsymbol{W}_{k+1} = \boldsymbol{W}_k - \delta * \nabla_{\boldsymbol{W}} E^{\boldsymbol{T}} \tag{7}$$

where the learning rate δ is usually chosen to be smaller than one, and $\nabla_{\boldsymbol{W}} E$ represents the gradient of the error function $E(\boldsymbol{W})$ with respect to $\boldsymbol{W}$. The weighting vector $\boldsymbol{W}$ is updated until $E(\boldsymbol{W})$ reaches the preset values.

III. Sensing Principle and Procedures

The observed normalized transmission power spectrum of an FBG can be represented by the following general form:

$$RT = S(f, T) \tag{8}$$

where RT is the detected normalized transmission power spectrum, f is the laser frequency, T is the temperature of the environment, and $S(\cdot)$ means the function mapping from (f, T) to the normalized transmission power spectrum RT. Obviously, mapping from (f, T) to RT is a multiple-to-one mapping, which is suitable for the ANN to learn. Therefore, we can utilize the learning ability of the ANN, denoted as $Sneu(\cdot)$, to approximate the function $S(\cdot)$. If $Sneu(\cdot)$ is sufficiently trained to approximate $S(\cdot)$ in a finite region Ω, then we can represent the right-hand side of (8) in the finite region Ω as follows:

$$RT = \{Sneu(f, T) | (f, T) \in \Omega\}. \tag{9}$$

According to (1), if we take f as M_1 and T as M_2, then we can use the modular ANN to form $Sneu(\cdot)$.

Since $Sneu(\cdot)$ replaces the normalized transmission power spectrum, $S(\cdot)$ and RT can be measured. So, based on (9), (f, T) may be obtained from RT. In order to make the computational process easier and more robust to handle, we convert (9) into a minimization problem instead of solving (9) directly. We define an objective function as follows:

$$J(f, T) = (RT - Sneu(f, T))^2. \tag{10}$$

The minimization algorithms such as the steepest descent method [20] can now be applied. In (10), $(RT - Sneu(f, T))^2$, with fixed f or T, is a good convex function around the solution of the other variable. This characteristic of (10) will enhance the accuracy of the solution. Here, we use the ANN to learn $S(\cdot)$, not only to take the advantage of the general ability of the ANN to overcome model mismatching between the theoretical design and the practical normalized transmission power spectrum profile of the FBG, but also to use the first order differentiability of the ANN.

In this paper, two FBG's, FBG_1 and FBG_2, are used to sense the frequency and temperature simultaneously [21], and two ANNS, $Sneu_1(\cdot)$ and $Sneu_2(\cdot)$, are employed to present the normalized transmission power spectra $S_1(\cdot)$ and $S_2(\cdot)$ for FBG_1 and FBG_2, respectively. In the following experiment,

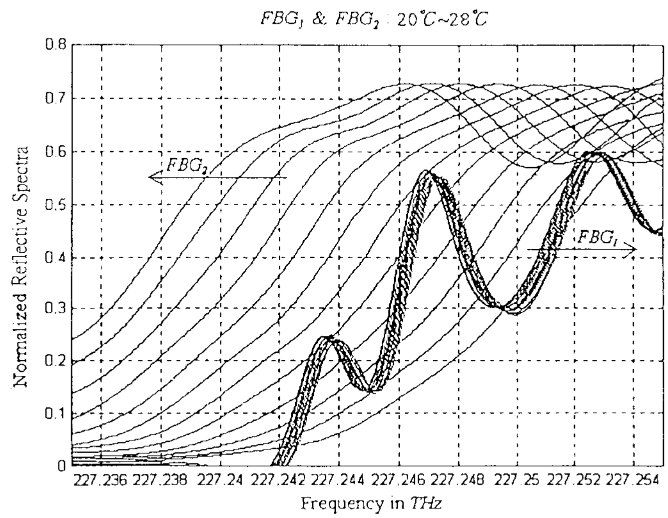

Fig. 4. The measured reflective spectra of two FBG's.

Authorized licensed use limited to: National Taiwan University. Downloaded on January 23, 2009 at 00:46 from IEEE Xplore. Restrictions apply.

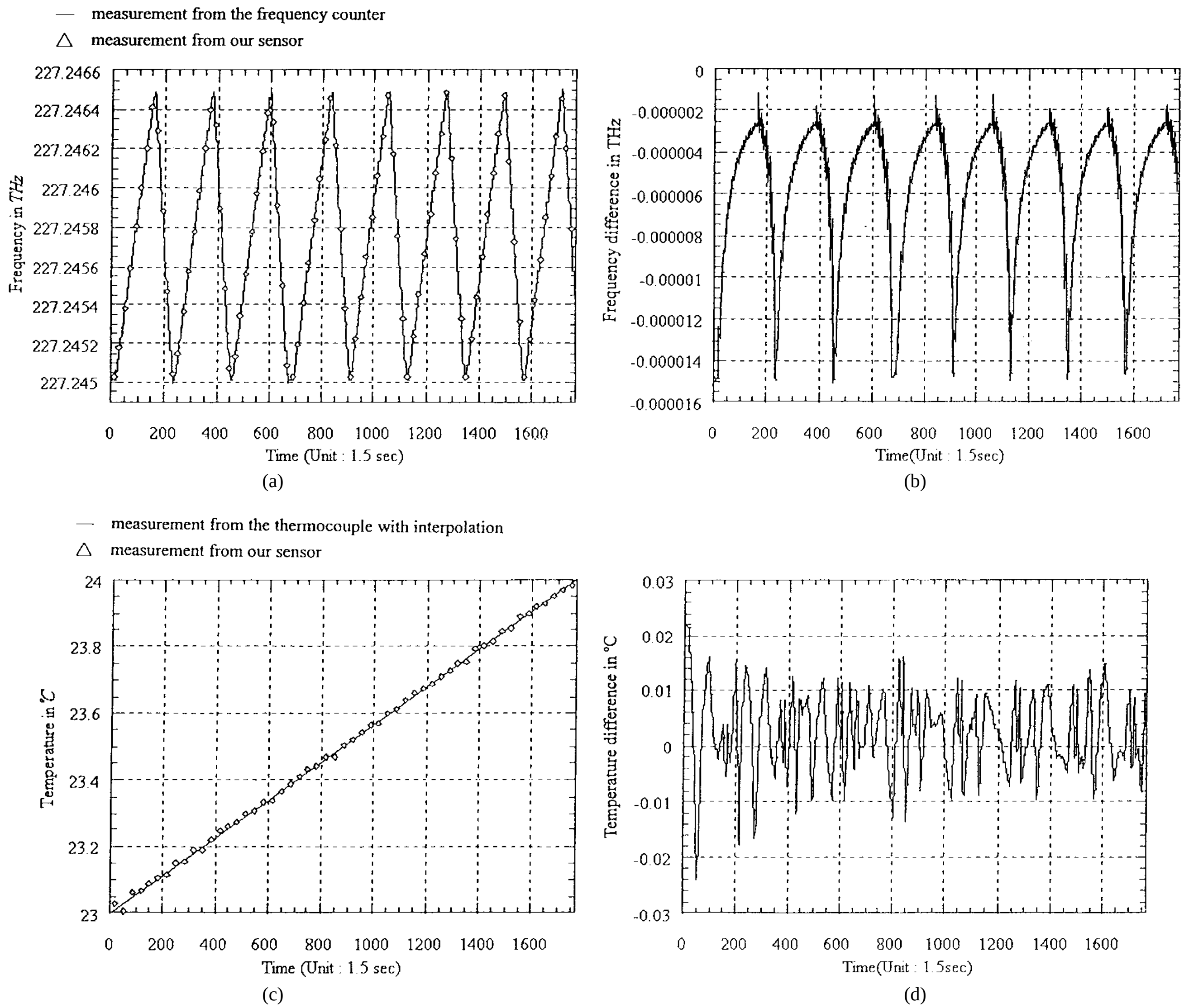

Fig. 5. (a) Frequency measurement with triangular driving laser. (b) Frequency measurement difference with triangular driving laser. (c) Temperature measurement with triangular driving laser. (d) Temperature measurement difference with triangular driving laser.

we measure two points of the normalized transmission power spectra (RT_1 for $S_1(\cdot)$ and RT_2 for $S_2(\cdot)$) at a fixed laser frequency. Then, we can use the minimization method to minimize the following objective functions sequentially for every incoming experimental data pair, RT_1 and RT_2. The one-variable objective functions are given by

$$J_f(f) = (RT_1 - Sneu_1(f,T))^2, \quad \text{with } T = T^* \tag{11}$$

and

$$J_T(T) = (RT_2 - Sneu_2(f,T))^2, \quad \text{with } f = f^* \tag{12}$$

where f^* and T^* are the solutions of minimizing (11) and (12). At each step of iteration, we take the last solutions f^*_{last} and T^*_{last} as the initial values for (11) and (12), respectively. Of course, the temperature variation can be estimated by such an iteration. Before starting the sensing procedure, we can initialize (f_o, T_o) and T^*_{last} intuitively. The whole procedure is illustrated in Fig. 2. The method used in this paper for resolving the laser light frequency and temperature simultaneously does not require a stabilized laser having a specified wavelength. This method can be used in any system with embedded narrow-linewidth lasers.

IV. Experimental Setup and Results

Fig. 3 shows the experimental setup of the high-resolution neural temperature sensor using two FBG's. We employ a diode-pumped Nd:YAG laser operating around 227.245 THz as a narrow-linewidth light source. The light is split into two branches by the coupler C_f and sent to a frequency counter and the coupler C_p which splits the light again into two branches, one for a coupler C_1, and the other for another coupler C_2, followed by the FBG's and two power detectors to detect the entering reference power. At the outputs of the FBG's, we use two other power detectors to detect the transmitted powers. We measure the reflective spectra with a power meter and frequency counter as shown in Fig. 4. As the temperature increases from 20 °C to 28 °C, the reflective spectra will shift in the opposite direction. Then, a microprocessor is used to calculate the detected normalized transmission power spectra

Authorized licensed use limited to: National Taiwan University. Downloaded on January 23, 2009 at 00:46 from IEEE Xplore. Restrictions apply.

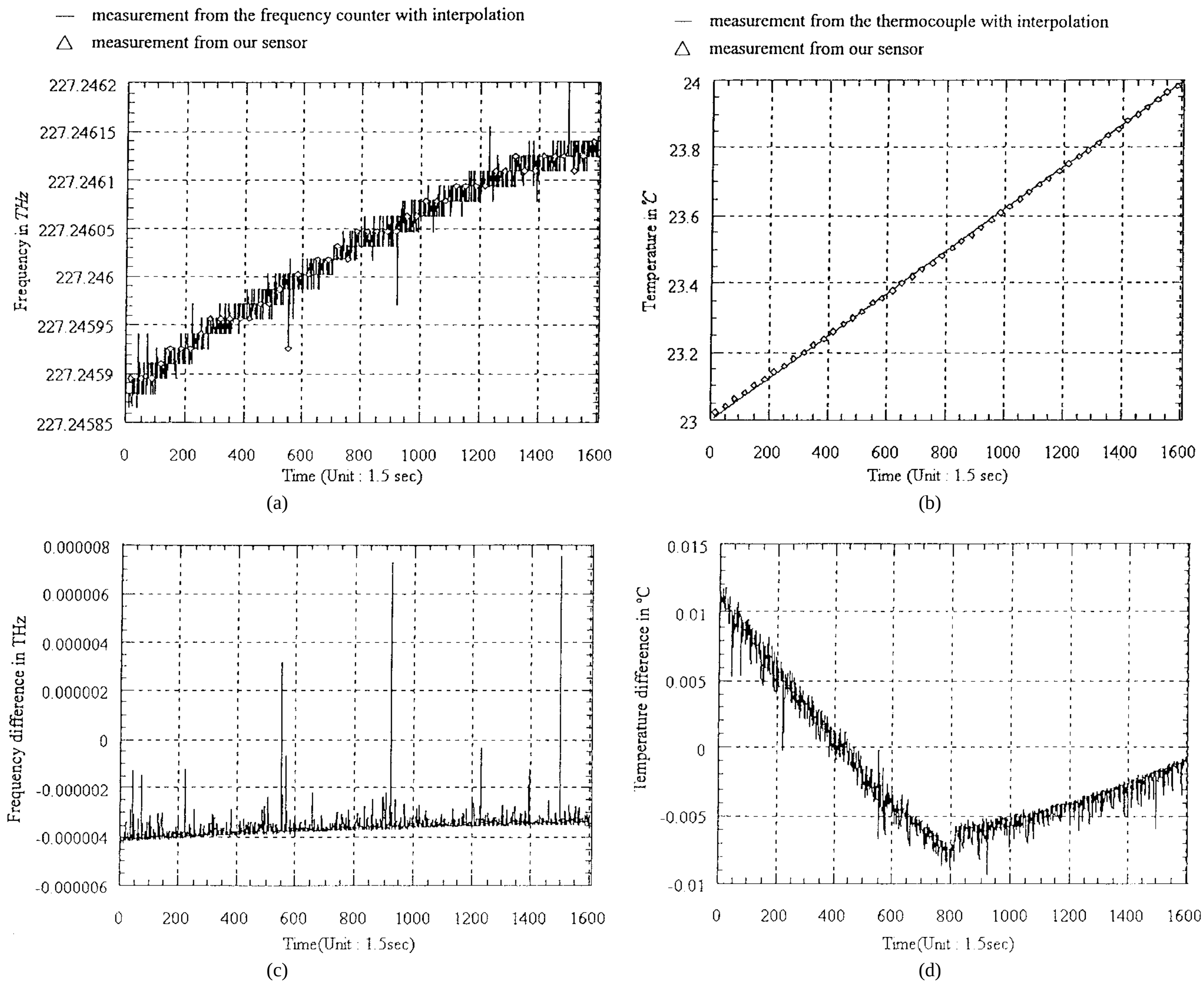

Fig. 6. (a) Frequency measurement with a free-running laser. (b) Temperature measurement with a free-running laser. (c) Frequency measurement difference with a free-running laser. (d) Temperature measurement difference with a free-running laser.

RT_1 and RT_2 for FBG_1 and FBG_2, respectively. We put FBG_1 in ambient air to detect the variation of frequency and place FBG_2 in a heat reservoir to detect the temperature variation.

During the measurement, we allow FGB_1 in the air at room temperature ($\sim$23.2 °C) and then increase the temperature of the heat reservoir including FBG_2. The accuracy of the temperature can exceed 0.01 °C, which is the best resolution of the electrical temperature probe used as a reference in this experiment. In order to improve the resolution of the reference, we continuously and steadily increase the temperature of the heat reservoir, thereby obtaining a linearly increasing temperature with respect to time. Subsequently, linear interpolation is applied to increasing the reference resolution, which is used for comparison with the measurement of our sensor.

To demonstrate the sensor, we first change the temperature of the heat reservoir steadily and electrically tune the optical frequency of the laser frequency periodically. The direct frequency readings from the frequency counter and the measured frequency from our sensor system are depicted in Fig. 5(a). It is seen that the difference, in which the periodic variation of the frequency difference is caused by the model mismatch between $Sneu_1(\cdot)$ and $S_1(\cdot)$ that is small, as shown in Fig. 5(b). The measured temperature values from the thermocouple (with interpolation) and our sensor system are plotted in Fig. 5(c), and the difference is again very small, as shown in Fig. 5(d). The rms errors of frequency and temperature are 6.0 MHz and 0.007 °C, respectively.

Next, we let the laser run without control and the optical frequency drift freely. The measured frequency and temperature are shown in Fig. 6(a) and (b). The measurement differences are presented in Fig. 6(c) and (d). It is observed that the rms errors for frequency and temperature are 4 MHz and 0.005 °C, respectively. With our experimental setup, the short-term (over one week) stability of the measurement has been studied. The frequency sensing stability can be maintained under 12 MHz by using a frequency counter (model no. MF9630A). Some spurious data measured by this frequency counter (solid line) as shown in Fig. 6(a), caused by repeated mechanical sweeping of the inteferometer in the frequency counter, should be ignored. Data measured by using our sensor yield the accurate results (triangle spot) shown in Fig. 6(a). Neglecting the spurious data, the long-term stability will be

Authorized licensed use limited to: National Taiwan University. Downloaded on January 23, 2009 at 00:46 from IEEE Xplore. Restrictions apply.

better than 4 MHz as shown in Fig. 6(c). Similarly, we studied the accuracy of temperature sensing as shown in Fig. 6(a) and (b). In fact, long-term stability of the sensing process can be achieved [22]. The temperature differences shown in Fig. 6(d) are induced by imperfect PID control of the heater and some environmental vibration sensed by the fiber sensor. In an uncontrolled environment, i.e., both optical frequency drifting and temperature changing freely, similar measured results can be obtained. This demonstrates that, based on the proposed structure of two FBG's and the modular ANN, a compact high-resolution and real-time temperature and frequency sensor is potentially achievable.

V. Conclusions

We have demonstrated a novel high-resolution temperature sensor employing a modular ANN and two FBG's. The optical transmitted power and the differentiability of the modular ANN are applied to resolve the optical frequency and temperature. A temperature measuring range over 8 °C is presented in this paper. According to our experiments, a temperature sensing range of at least 20 °C is achievable. The sensing range can be extended by designing the thermal expansion coefficients of the two FBG sensors for a wider temperature range.

In our experiment, we exploit the modular ANN with some advantages. The modular model can deal with physical parameters and improve the accuracy of the modeling. It also reduces the number of network connections. With the network sparsely connected, we can improve the computational speed and generalization ability. At the same time, interference from irrelevant or redundant learning can be avoided. When the nonlinear mapping changes, the modular ANN can be modified and updated easily, because only a portion of the whole network is required to retrain. As a matter of fact, hybrid models, which have modules of varying characteristics, can be developed to suit specific applications.

The relationship among the detected power spectrum, laser frequency, and temperature is suitable for the ANN to learn, because our sensing scheme does not suffer the one-to-many mapping problem. Based on the generalization ability and required small training region of the ANN, the neural network can be trained easily. Meanwhile, the ANN can also compensate for the modeling error of the spectrum profile. Our sensing scheme does not need the information of the entire power spectrum or phase detection. That makes the measuring procedure faster and more efficient. It is expected that this sensor can combine with multiplexing schemes, such as wavelength, time, and space division multiplexings.

References

[1] Y.-J. Rao, "In-fiber Bragg grating sensors," *Meas. Sci. Technol.*, vol. 8, pp. 355–375, 1997.

[2] K. O. Hill and G. Meltz, "Fiber Bragg grating technology fundamentals and overview," *J. Lightwave Technol.*, vol. 15, pp. 1263–1276, Aug. 1997.

[3] S. M. Melle, K. Liu, and R. M. Measures, "A passive wavelength demodulation system for guided-wave Bragg grating sensors," *IEEE Photon. Technol. Lett.*, vol. 4, pp. 516–518, 1992.

[4] M. A. Davis and A. D. Kersey, "All fiber Bragg grating strain sensor demodulation technique using a wavelength division coupler," *Electron. Lett.*, vol. 30, pp. 75–78, 1994.

[5] ——, "Matched-filter interrogation technique for fiber Bragg grating arrays," *Electron. Lett.*, vol. 31, pp. 822–823, 1995.

[6] A. D. Kersey, D. A. Tackson, and M. Corke, "A simple fiber Fabry-Perot sensor," *Opt. Commun.*, vol. 45, pp. 71–74, 1983.

[7] A. D. Kersey and T. A. Berkoff, "Fiber-optic Bragg-grating differential-temperature sensor," *IEEE Photon. Technol. Lett.*, vol. 4, pp. 1183–1185, Oct. 1992.

[8] Y. J. Rao, D. A. Jackson, L. Zhang, and I. Bennion, "Dual-cavity interferometric wavelength-shift detection for in-fiber Bragg grating sensors," *Opt. Lett.*, vol. 21, pp. 1556–1558, 1996.

[9] W. Ecke, J. Schauer, K. Usbeck, R. Willsch, and J. P. Dakin, "Improvement of the stability of fiber grating interrogation systems using active and passive polarization scrambling devices," in *Proc. 12th Optical Fiber Sensor Conf.*, Williamsburg, VA, 1997, pp. 484–487.

[10] K. Usbeck, W. Ecke, V. Hagemann, R. Mueller, and R. Willsch, "Temperature referenced fiber Bragg grating refractometer sensor for on-line quality control of petrol products," in *Proc. 13th Optical Fiber Sensor Conf.*, Kyongju, Korea, 1999, pp. 163–166.

[11] W. J. Bock, E. Porada, and M. B. Zaremba, "Neural processing-type fiber-optic strain sensor," *IEEE Trans. Instrum. Meas.*, vol. 41, pp. 1062–1066, 1992.

[12] P. Dacosta, C. Kordich, D. Williams, and J. B. Gomm, "Estimation of inaccessible fermentation states with variable inoculum sizes," *Artif. Intell. Eng.*, vol. 11, pp. 383–392, 1997.

[13] S. Aisawa, K. Noguchi, and T. Matsumoto, "Neural processing type displacement sensor employing multimode waveguide," *IEEE Photon. Technol. Lett.*, vol. 3, pp. 394–396, Apr. 1991.

[14] H. Eren, C. C. Fung, K. W. Wong, and A. Gupta, "Artificial neural networks in estimation of hydrocyclone parameter d50c with unusual input variables," *IEEE Trans. Instrum. Meas.*, vol. 46, pp. 908–912, 1997.

[15] K. Zhang, C. Butler, Q. Yang, and Y. Lu, "A fiber optic sensor for the measurement of surface roughness and displacement using artificial neural networks," *IEEE Trans. Instrum. Meas.*, vol. 46, pp. 899–902, 1997.

[16] K. Hornik, M. Stinchcombe, and H. White, "Multilayer feedforward networks are universal approximators," *Neural Networks*, vol. 2, pp. 359–366, 1989.

[17] L. A. Zadeh, "Fuzzy sets," *Inform. Control*, vol. 8, pp. 338–353, 1965.

[18] ——, "Outline of a new approach to the analysis of complex systems and decision processes," *IEEE Trans. Syst., Man, Cybern.*, vol. 3, pp. 28–44, 1973.

[19] F.-C. Chen, "Back-propagation neural networks for nonlinear self-tuning adaptive control," *IEEE Control Systems Mag.*, pp. 44–48, 1990.

[20] R. L. Burden and J. D. Faires, *Numerical Analysis*, 6th ed. New York: PWS, 1997.

[21] S.-L. Tsao and J. Wu, "Highly accurate temperature sensor using two fiber Bragg gratings," *IEEE J. Select. Topics Quantum Electron.*, vol. 2, pp. 894–897, 1996.

[22] S.-L. Tsao, J. Wu, and B.-C. Yeh, "A fiber Bragg grating temperature sensor with artificial neural networks," in *Proc. 13th Int. Conf. Optical Fiber Sensors*, Kyongju, Korea, 1999, pp. 438–441.

Shyh-Lin Tsao (S'92–M'96) received the B.S. degree in physics from Fu-Jen University and the M.S. degree in the Institute of Optical Sciences from National Central University, Taiwan, R.O.C., in 1987 and 1989, respectively, and the Ph.D. degree in electrical engineering from National Taiwan University, Taipei, Taiwan, R.O.C., in 1995.

He was with the Department of Electronic Engineering of ST. John's and ST. Mary's Institute of Technology and Fu-Jen University between 1995–1997 as an Associate Professor. In 1997, he joined the Department of Electrical Engineering of Yuan Ze University, Chung-Li, Taiwain, R.O.C., as an Associate Professor. He served as the chairman of the 1997 Conference on Communication Engineering (CCE'97). He has also served as the "Communication System" section chairman of 1998 Fourth Computer and Communication Conference and the "Statistical Communication Theory and Optical Communication" section chairman of 1998 National Symposium on Telecommunications (NSTC'98). His research interests include optical fiber communication systems, fiber sensors, integrated optics, optical interconnection, optical signal processing, nonlinear optics, microwave circuits, CATV, and high-speed communication networks.

Dr. Tsao is a member of the Optical Society of America, the Society of Photo-Optical Instrumentation Engineers, and the American Association for the Advancement of Science. His name is listed in *Who's Who in the World* and *Who's Who in Finance and Industry*.

Authorized licensed use limited to: National Taiwan University. Downloaded on January 23, 2009 at 00:46 from IEEE Xplore. Restrictions apply.

Jingshown Wu (S'73–M'78) received the B.S. and M.S. degrees in electrical engineering from National Taiwan University, Taipei, and the Ph.D. degree from Cornell University, Ithaca, NY, in 1970, 1972, and 1978, respectively.

He joined Bell Laboratories in 1978, where he worked on digital network standards and performance, and optical fiber communication systems. In 1984, he joined the Department of Electrical Engineering, National Taiwan University, as Professor as was the Chairman of the Department from 1987 to 1989. He was also the Director of the Communication Research Center, College of Engineering of the University from 1992 to 1995. From 1995 to 1998, he was the Director of the Division of Engineering and Applied Science, National Science Council, Taiwan. Currently, he is a Professor at the same university. His research interests include optical fiber communications, communication electronics, and computer communication networks.

Prof. Wu is a member of the Chinese Institute of Engineers, the Optical Society of China, and the Insitute of Chinese Electrical Engineers. He is the Chairman of the IEEE Taipei Section.

Bih-Chyun Yeh was born in Taipei, Taiwan, on November 22, 1973. He received the B.S. and M.S. degrees in electrical engineering from National Taiwan University, Taipei, in 1996 and 1998, respectively.

He is interested in optical sensors, optical communications, and wavelength-division multiplexing technology.

Authorized licensed use limited to: National Taiwan University. Downloaded on January 23, 2009 at 00:46 from IEEE Xplore. Restrictions apply.